

Structural, Optical, Morphological and Electrical Properties of V₂O₅ Nanorods by Wet Chemical Method

R.Thangarasu¹, K.Tamilselvan², O.N. Balasundaram³,

^{1,2,3} Dept of Physics

^{1,2,3} PSG College of Arts & Science, Coimbatore- 641 014, Tamilnadu, India

Abstract- In this study, V₂O₅ nanoparticles prepared by wet chemical method. The achieve of preparation and characterization by XRD, HR-TEM, UV, PL, FTIR, DC conductivity studies. The X-ray diffraction analysis revealed that the prepared sample annealed at 600° C for 1 hrs. This exhibited that orthorhombic phase of V₂O₅ nanorods. The powders are characterized for optical properties by studying the optical absorption spectra in the wavelength range 200-1000 nm at room temperature using UV-vis spectrometer. The V₂O₅ nanorods produced by this technique are single crystalline and could emit intense visible light at room temperature, possibly due to some defects such as oxygen vacancies which got involved during growth. FTIR spectrum confirmed that the presence of V₂O₅ function group and the formation of V-O bond system. The HR-TEM images dense, smooth and random distribution of V₂O₅ nanorods. The DC electrical conductivity was studies as a function of temperature which indicated the semiconductor nature.

Keywords- V₂O₅, XRD, sol-gel, Optical, nanorods, conductivity

I. INTRODUCTION

Vanadium pentoxide (V₂O₅) due to its excellent and unique physical and chemical properties as a semiconductor material. V₂O₅ is the saturated (highest oxidation state) oxide, and therefore the most stable one, in the V–O system [1]. Vanadium occurs as a single valence in oxidation states from V²⁺ to V⁵⁺, in the form of different phases (VO, VO₂, V₂O₃, V₄O₉ and V₂O₅) and a number of mixed-valence oxides (V₆O₁₃, V₁₀O₂₄). Though the presence of various phases, single or multiple valence states and different layered structures (vanadium oxides) can be described from the application point of view, a single phase V₂O₅ is more suitable and its practical importance of great interest in different fields of science and technology. Among them V₂O₅ is mostly studied and it is considered to be a prominent n-type semiconductor with wide direct band gap (2.42 eV) [2]. And attracts continuing attention owing to its

great potential in a wide variety of scientific and technological applications in recent years. They find extensive applications in areas such as high energy lithium batteries [3], catalysis [4], solar cells [5] and field effect transistors (FETs) [6]. Now days, one-dimensional (1D) - V₂O₅ nano structures such as nano wires, nano belts nano spindle and nano rods gain notice considerably due to their unique properties towards electronic and optoelectronic application. Among the 1D- V₂O₅ is perhaps the most studied, owing to its features like in expensive preparation, high stability and the significantly large energy density. During the past decades, a variety of methods such as reverse- micelles synthesis [7], sol-gel method [8], hydrothermal [9], chemical vapor deposition [10], thermal-decomposition [11], pulsed laser deposition [12] and electro-spinning [13] are commonly used to prepare 1D- V₂O₅ nano structures. Compared with these methods, sol-gel synthetic route holds the advantage of easier control of the morphological parameters of nano materials and does not require any sophisticated equipment's. Avansi et al. recently reported an environmentally one step hydrothermal route for synthesis of V₂O₅ nanostructure [14]. Muster et al. studied the electrical transport mechanism route for synthesis of V₂O₅ nanofibers in detail [15]. Ferrer-anglada et al. analysed the current-voltage (I-V) Characteristics and electrical resistance was measured on V₂O_{5-x} polyaniline nanorods [16]. This work, we studied the effect of temperature on structural and optical properties of 1D- nanoparticles by the sol-gel method. Synthesis of V₂O₅ nanorods by this method exhibits much better optical, morphological and electrical properties than commercial nanosized V₂O₅. Further the nanoparticles were characterized by various techniques and the characterization results are discussed in details.

II. EXPERIMENTAL PROCEDURE

All of the chemicals were used in the experiment were of analytical reagent (AR) grade and used without any further purification. The ammonium meta vanadate (NH₄VO₃), hydrogen peroxide (H₂O₂), nitric acid (HNO₃), Polyvinylpyrrolidone (PVP), purchased from Merck company,

was used as the precursor materials for synthesis of V_2O_5 nanoparticles by wet chemical method. The flow chart of the preparation of V_2O_5 nanoparticles is shown in Fig. 1. In a typical synthesis procedure, an appropriate amount of ammonium meta vanadate (NH_4VO_3) was dissolved in deionised water and stirred for 10–30 min at room temperature. In the aqueous solution contains a milky white color was precipitated then a given amount of 10ml 35% H_2O_2 was added, quickly the milky white color changed to light pale yellow shade. Upon an introduction of aliquot concentrated Hcl acid was into the system, the color of the reaction mixture changed from pale yellow to dark orange color [17]. Finally, a desired amount of Polyvinylpyrrolidone (PVP) was added into concoction solution under vigorous stirring for 24h. In the resulting pale yellow gel form was filtered, washed with deionised water and absolute ethanol, and acetone dried at $90^\circ C$ for 6h to get as-prepared sample. Then dried product was transferred to a silicon crucible for purpose of sintering and placed in muffle furnace used at temperatures, say $600^\circ C$ for 1 h till yellow colored V_2O_5 nano-particles were obtained.

III. CHARACTERIZATION TECHNIQUES

The crystal structural characterization of the V_2O_5 nanorods was performed by X-ray diffraction using a Bruker AXS D8 advance diffractometer with Cu-K α radiation source $\lambda=1.5406 \text{ \AA}$. The absorption spectrum studies are also done using UV–vis–NIR spectro photo meter between 200 and 1000 nm (Jasco V-570). The Spectro fluometer spectrum is examined by the instrument model of Jobin Yvon Fluoromax of 185–900nm. The Fourier transform infrared (FT-IR) (Perkin Elmer 100) is used to record the spectra range from 400 to 4000 cm^{-1} with are solution of 4 cm^{-1} . The structure and morphology of nanorods were examined using High-Resolution Transmission Electron Microscopy (JEOL JEM-2100, HRTEM, and Japan). I-V Characterized were studies (in pellet form) with using the help of Keithly Electrometer 6517B.

IV. RESULT AND DISCUSSION

4.1 XRD-Analysis

Fig.1 (a) demonstrates the xrd profiles of the V_2O_5 nanoparticles prepared in surfactants solutions. Xrd pattern of PVP capped V_2O_5 nanorods. No excess peaks, which indicate that all the precursors have been completely decomposed and no other complex products were formed. All the diffraction peaks are indexed with the pure orthorhombic phase of V_2O_5 nanoparticles with the lattice parameters $a=11.207 \text{ \AA}$, $b=3537 \text{ \AA}$ and $c=4.397 \text{ \AA}$ (jcpds Card No: 41-1426 space group Pmmn) without any impurity peaks. Furthermore, the

crystalline size can be estimated to be 20-55nm, for pure V_2O_5 by using the debye-scherrer formula. The average grain size of calculation at $550^\circ C$ were calculated to be 21.68 nm, from the (200), (001), (101), (110), (301), (011), and (310) peaks using the Debye scherrer equation

$$D = \frac{k\lambda}{\beta \cos \theta} \text{-----(1)}$$

$$d = \frac{n\lambda}{2 \sin \theta} \text{-----(2)}$$

Where d is the crystallite size, λ is the X-ray wavelength (1.54 \AA), β is full width at half maximum of the high intensity peak and θ is Bragg's diffraction angle in degrees. It is clear that of V_2O_5 crystalline nature in calcinations temperature at $550^\circ C$ for crystallinity nature to that of $550^\circ C$ probably due to the formation of structural defects. Notably the sample annealed at $550^\circ C$ producing a significant improvement in crystallinity, showing more strong and sharper Diffraction peaks as compared to the other sample the number of diffraction line increase in V_2O_5 orientations with temperature increase in the crystallite size [18].

The difference in the estimated crystalline size indicates that there are some differences in size and morphology of the V_2O_5 nanoparticles.

The dislocation density which represents the amount of defect in the samples is determined from the formula (3)

$$\delta = \frac{1}{D^2} \text{-----(3)}$$

$$\varepsilon = \frac{\beta \cos \theta}{4} \text{-----(4)}$$

Where D is the grain size. The dislocation density decreases with increasing annealing temperature which may be due to decrease in concentration of lattice imperfections [19]. The influence of particle size on lattice parameter also noticed from XRD pattern. The particle size increases, the value of lattice parameter decreases as shown in Fig.1 (a) and

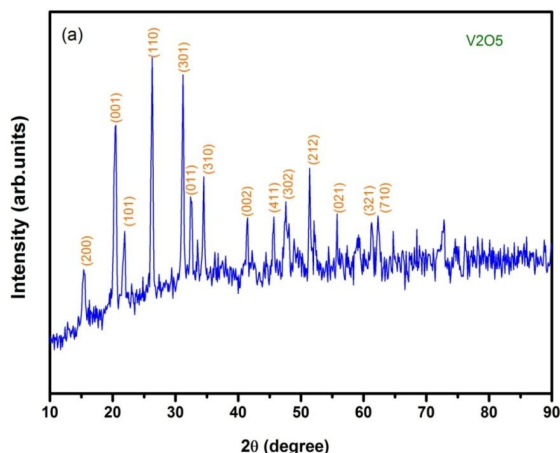


Fig. 1 (a) XRD structure of V₂O₅ sample at 600°C temperature

Table: 1 Structural Parameters of V₂O₅ nanorods

| Material | 2theta (deg) | (hkl) | FWHM | Lattice parameters | Crystallite size | Dislocation Density (lines/m ²) | Micro strain(ε) (10 ⁻³) |
|-------------------------------|--------------|-------|--------|--------------------|------------------|---|-------------------------------------|
| V ₂ O ₅ | 21.50 | (101) | 0.5617 | a =11.2079 | 14.39 nm | 0.0694 | 0.1379 |
| | 26.50 | (110) | 0.3035 | | 26.88nm | 0.0372 | 0.0738 |
| | 31.60 | (400) | 0.2795 | b =3.5370 | 29.53nm | 0.0338 | 0.0670 |
| | 38.50 | (401) | 0.0764 | | 11.01 nm | 0.0908 | 0.0180 |
| | 40.50 | (311) | 0.3183 | c =4.3978 | 26.60nm | 0.0375 | 0.0746 |

Table (1). It is seen from Fig. 1(a), the dislocation density and strain are both decrease when the annealed temperature 600°C. A sharp decrease dislocation density and strain improve the crystallinity of the V₂O₅ nanoparticle is calculated (101) plane.

4.2 UV –Visible Spectroscopy

The UV-visible absorption spectrum of annealed at 600°C of V₂O₅ nanorods is shown in the Fig. 2(a). It can be seen that the excitonic absorption peak of V₂O₅ samples appear around 472.4 nm (E_g =2.64 eV) and it is shows a blue shift in comparison with the bulk V₂O₅ (E_g = 2.34 eV), Which may be ascribed to the quantum confinement effect due to electronic transition from occupied 2p bands of oxygen to unoccupied 3d bands of vanadium [20].

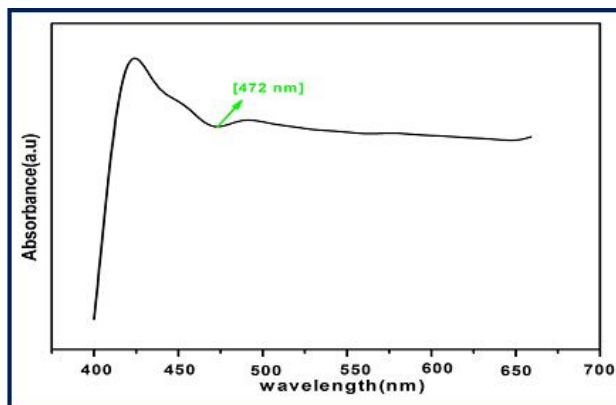


Fig. 2(a) UV–visible absorption spectra of V₂O₅ nanoparticle annealed at 550°C.

It is well-known that the band maxima of the charge transfer transition of O →Vⁿ⁺ depends on the number of oxygen atoms surroundings central vanadium ion [21]. Therefore, V⁵⁺ in tetrahedral coordination absorbs in the range 240-350 nm, in square pyramidal coordination at 350-450 nm and in octahedral coordination at 450-600nm. In this spectrum shows a weak band at around 472.4 nm which can be attributed to lower energy charge transfer to V⁵⁺ species in octahedral coordination. In the figure it can be observed clearly from the absorbance of the samples decreases slightly with increase in annealing temperature. Furthermore, a red-shift is observed in the characteristics absorption peak of V₂O₅, the optical band gap values of the V₂O₅ sample annealed at 600°C temperature to be about 2.64 eV that agrees with bulk of the band gap.

4.3 Photoluminescence spectroscopy

The optical properties of V₂O₅ nanorods, we carried out PL measurements at room temperature. The PL emission spectra of the V₂O₅ at 550°C annealing temperature are shown in Fig.3 (a). In intact case, it consists of strong blue green emission peak at 435 nm which is originated from there combination of free excitations.

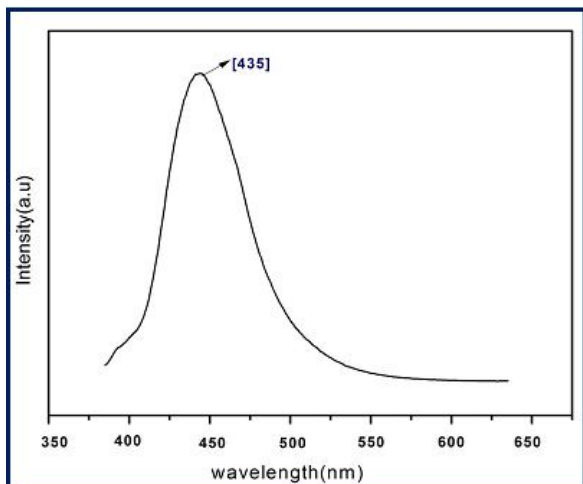


Fig. 3 (a). Photoluminescence spectrum of V₂O₅ annealed at 600 °C.

The luminescence at 435 nm may be considered to be related to the signal ionized oxygen vacancy due to the defect in V₂O₅. The broad emission band revealed in the visible region in our samples is due to the super position of blue-green emission. It was reported that the oxygen vacancies are responsible for the green emission are mainly located at the surface [22]. As the temperature increase, will be the positions are basically unchanged but the intensity of peak increase which may be attributing to the increase in grain size and crystallinity. The UV and blue-green emission of V₂O₅ nanorods have been broadly studied and the mechanism is also clearly known.

4.4 FTIR-Analysis \

The FI-IR spectrum of the V₂O₅ nanoparticles treated at 600°C is shown in Fig. 4(a) the analysis of spectrum contains very broad and strong absorption band centered at 3437 cm⁻¹ due to the stretching vibration of the O–H bond. Two sets of vibrational peaks observed at 2934, 2403 cm⁻¹ and 1659,1432 cm⁻¹ are related to the characteristic bands of symmetric stretching and scissoring (bending) modes of C–H group, respectively. The absorption peaks at 1741 and 1633 cm⁻¹ are due to the stretching vibration modes of C=O group. The V₂O₅ samples exhibits three main vibration modes in the 600–1020 cm⁻¹ region. The terminal oxygen symmetric stretching mode (ν_s) of V=O, the bridge oxygen asymmetric and symmetric stretching modes (ν_{as} and ν_s) of V–O–V are observed at 1017, 824 and 606 cm⁻¹, respectively [23].

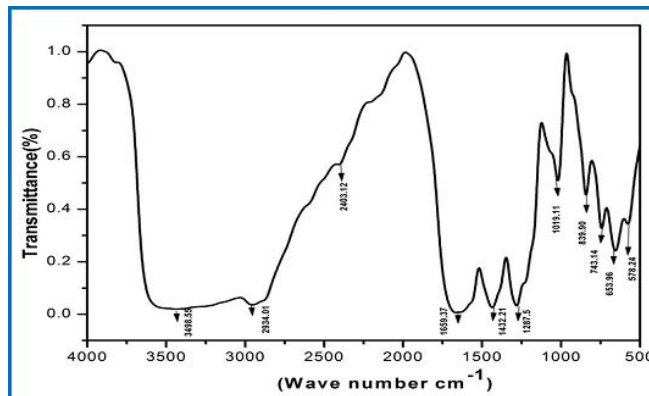


Fig. 4 (a). FT-IR Spectrum of V₂O₅ nanorods for chemical nature of the bonds

In the figure, the V₂O₅ samples annealed at 600°C, the organic bands diminished. It can be deduced that the crystal phase is improved at 600°C, as comparatively a lower annealing temperatures. The organic bands slowly decompose with increasing temperature, so that the crystallization process is essentially complete at 600°C.

4.5 TEM Analysis

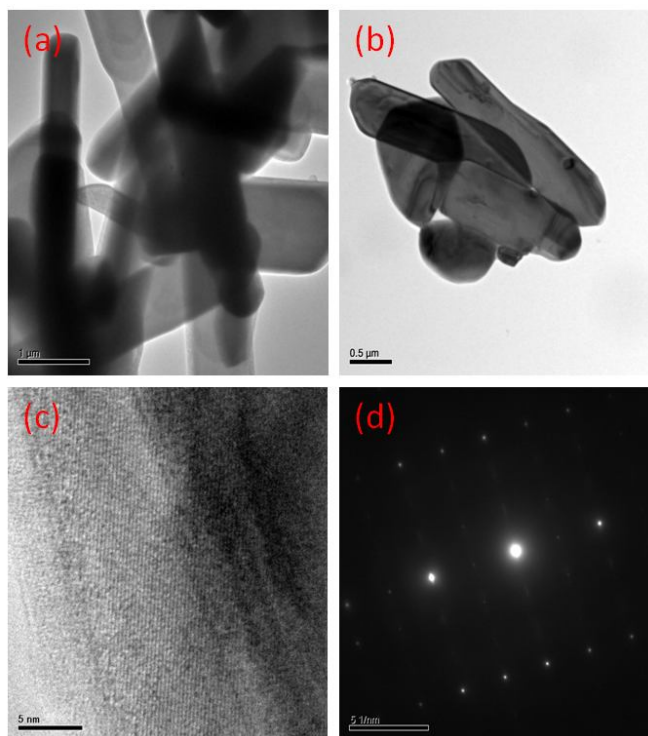


Fig. 5 HRTEM images of (a-b) V₂O₅ nanorods at annealing temperature at 600 °C (c) fringes of (001) plane with V₂O₅ (d) single crystalline V₂O₅ nanorods with SAED pattern.

Fig. 5(a-d) shows the TEM images V₂O₅ sample annealed at 600°C, which clearly indicated that formation of large size microrod particles. The average size and length of

individual microrods are about 45-90 nm and 2-3µm, which is in agreement with the SEM result. We suggest that the nanorods could be grown from the well defined faced end to the hexagonal face end, the HRTEM lattice fringes images shown in Fig 5 (c). reveals that the nanorods possess a single crystal hexagonal face structure without dislocations and stacking faults. The fringes images also confirms that the nanorods grow along the (002) direction with a lattice spacing of about 2.14Å indicating that the V₂O₅ nanorods is single crystalline in nature. The selected area electron diffraction (SAED) pattern presented in shown on Fig. 5(d) bright spot in the sample, we can see the images of orthorhombic structure of V₂O₅. In this regard, a significant transition of SAED pattern for the crystalline nature of V₂O₅ sample at 600°C is observed [24].

4.6 DC Conductivity

I-V characteristics studs low to high level temperatures shown on Fig 6(a) and are found to be linear behaviours from lower temperature. The current in lower voltage range (1-10v) from 30-130°C and in higher voltage range they deviation from the low temperature are indicated ohmic behaviour. It is also evident from Fig. 6 (a). The applied voltage are increase with higher temperature .it can be seen that I-V characteristics deviates from non-ohmic behaviour and slowly the resistance goes on decreasing. In order to study the qualitatively this behaviour of material for whole mechanism could be divided into two parts. First one is related to the lower and higher temperature dependence of conductivity and resistance for samples under test [25]. The second is related with the deviation of ohmic behaviour towards non-ohmic behaviour of I–V characteristics at higher voltages applied across the sample

The conductivity and resistivity of the prepared samples are calculated as from the equation

$$\sigma = \frac{1}{\rho} = \frac{It}{VAS/cm} \tag{5}$$

Where, I is the current, V is the applied voltage t-is the thickness of the pellet and A-is the area of the pellet, in order to investigate the rectifying behaviour of the V₂O₅ Nanorods. I-V characteristic are obtained by connecting Keithley electrometer to the two probe setup.

$$\rho = \frac{AR}{l} \tag{6}$$

Where, ρ is the resistivity, R is the resistance, A is the cross sectional area, and l is the inter-probe distance, the

conductivity is computed from have the relation $\sigma = \frac{1}{\rho}$, where σ-is the conductivity

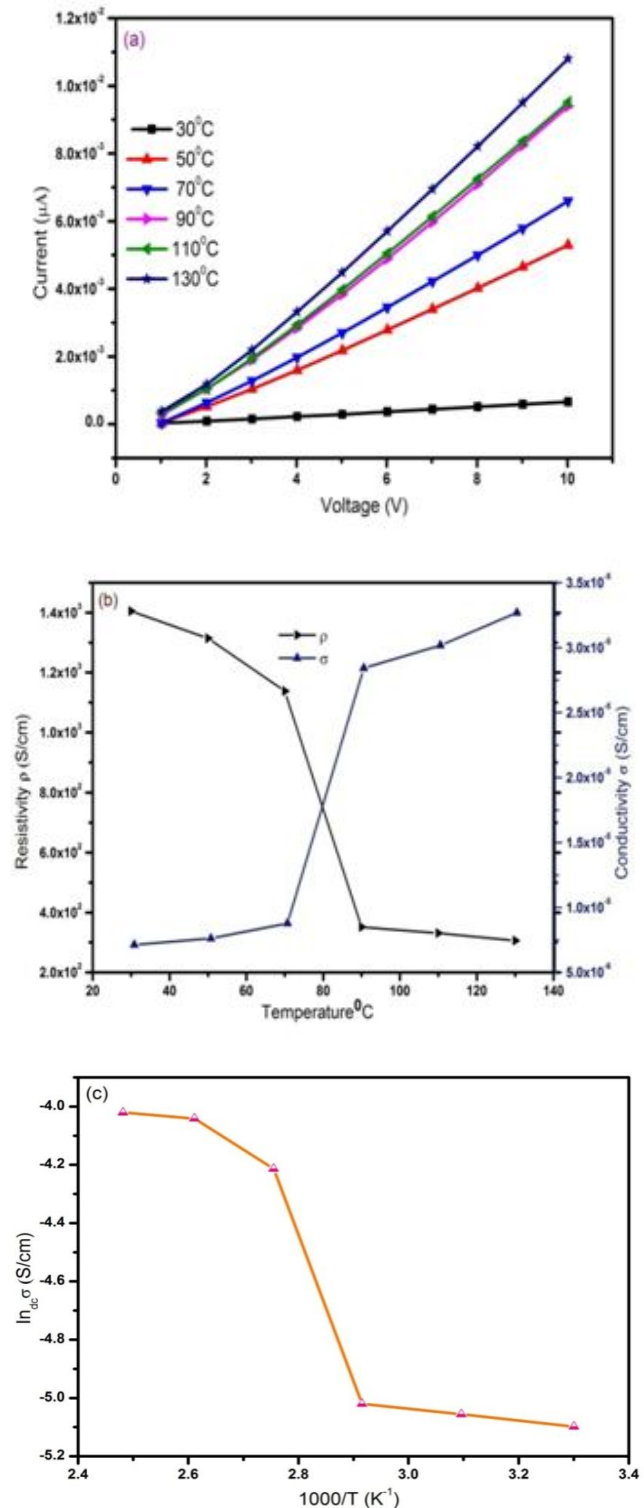


Fig. 6 (a-c) I-V Characteristics (a) V₂O₅ (b) Resistivity decrease and conductivity increase of V₂O₅ nanorods (c) activation energy of ln S dc (S/cm) Vs.103/T K⁻¹

The calculated for conductivity and resistivity are listed in the Table (2). The conductivity is found to be in the range 7.87×10^{-6} to $1.34 \times 10^{-5} \text{ S cm}^{-1}$ for different temperature 30-130°C. It is clear from Fig. 6 (b) the resistivity decrease with temperature which shows the semiconducting behaviour of the V_2O_5 nano rods. The conductivity increase show to opposite resistivity decreases, show resistivity in order to V_2O_5 , was $10^3 \text{ } \Omega/\text{cm}$, at 600°C for V_2O_5 nanorods [25].

Table. 2 Electrical parameters of the V_2O_5 nanorods

| Material | Resistivity (ρ) $\Omega \text{ cm}^{-1}$ | Conductivity (σ) S/cm^{-1} | Activation energy (E_a) eV |
|------------------------|--|---|-----------------------------------|
| V_2O_5 | 1.34×10^3 | 7.87×10^{-6} | 0.185 |

The values are in good agreement with the reported values. This may be due to the surfactants of exposed for the maximum solubility in V_2O_5 host lattice, more grain size boundary segregation of impurities that occurring as dispersion of charge carriers, the calculated as conductivity and resistivity parameter are listed in Table (2). The activation energy are calculated from the Arrhenius relation

$$\sigma = \sigma_0 \exp[-E_a/2K_B T] \quad (7)$$

Where, σ_0 is the pre exponential factor, E_a is the activation energy, K_B is the Boltzmann constant and T is the absolute temperature. The activation energy of the V_2O_5 for surfactants as V_2O_5 have been used as calculated from the slope of the plot $\log_{10} \sigma \text{ (S/cm) vs. } 1000/T \text{ (K}^{-1}\text{)}$ in the Fig. 6(c). Shows in the slope value determination plot for the V_2O_5 nanorods prepared at 600°C . The activation energy estimated for PVP surfactants have been listed in the table (2) the increase of PVP from 0.185 eV are present [26]. The activation energy value (0.27eV) due to the lower ionic size of the V_2O_5 nanorods that could be 0.185eV the values are in good agreement with the reported values.

V. CONCLUSION

V_2O_5 nanorods have been successfully prepared by wet chemical method. The XRD result revealed that the product is orthorhombic phase in nature. The blue shift observed in the UV-visible spectrum is the typical signature of quantum confinement effect in V_2O_5 nanorods. The PL spectra of V_2O_5 nanorods reveal that the blue-green emission with intensity related to the structural defects. FTIR spectrum

conformed that the presence of V_2O_5 functional groups and the formation of V-O bond. HRTEM image reveals clearly the formation of hexagonal nanorods when the V_2O_5 nanorods at 600°C . The dc electrical conductivity was studied as a function of temperature which indicated the semiconducting nature. Here, on that resistivity decrease and conductivity increase with activation energy studied for the V_2O_5 nanorods.

VI. ACKNOWLEDGEMENTS

Authors wish to express their sincere thanks to the UGC-Rajiv Gandhi National fellowship at New Delhi.

REFERENCE

- [1] F.J. Morin, Phys. Rev. Lett, 3 (1959) 34-35.
- [2] H.N. Van, D. Lichtman, J. Vac. Sci. Tech, 18 (1981) 49-53.
- [3] T. Kudo, Y. Ikeda, T. Watanabe, M. Hibino, M. Miyayama, H. Abe, K. Kajita, Solid State Ion. 153 (2002) 833-841.
- [4] A. Legrouri, T. Baird, J.R. Fryer, J. Catal. 140(1993)173-183.
- [5] J.Wu, Y. Zhanq, Y.He, C.Liu, W.Guolt, S.Ruan, J.Nanosci. Nanotechnol. 14(2014) 4214-4217.
- [6] G.T.Kim, J.Muster, V. Krstic, Y.W. Par, S. Roth, M. Burghard, Appl. Phys. Lett. 76 (2000) 1875-1877.
- [7] N. Pinna, M. Willinger, K. Weiss, J. Urban, R. Schlogl, Nano. Lett. 3 (2003) 1131-1134.
- [8] Z. Wang, J. Chen, X. Hu, Thin Solid Films. 375(2000)238-241.
- [9] N.C.S. Vieira, W. Avansi, A. Figueiredo, C. Ribeiro, V. R. Mastelaro, E. Guimaraes, Nano. Res. Lett. 7(2012)310-314
- [10] Yawning, Q. Su, C. H. Chen, M. L. Yu, G. J. Han, G. Q. Wang, K. Xin, W. Lan, X. Q. Liu, J. Phys. D: Appl. Phys. 43(2010)183001-185402.
- [11] A. Pan, J. G. Zhang, Z. Nie, G. Cao, B. W. Arey, G. Li, S. Q. Liang, J. Liu, J. Mater. Chem. 20(2010)9193-9199.
- [12] C. Ramana, R. J. Smith, O. M. Hussain, C. M. Julien, Mater. Sci. Eng. B 11(2004)218-225.
- [13] P. Viswanathamurthi, N. Bhattarai, H. Y. Kim, D. R. Lee, Scr. Mater. 49(2003) 77-581.
- [14] W. Avansi, C. Ribeiro, E. R. Leite, V. R. Mastelaro, Crystal Growth and Design 9 (2009) 3626-3631.
- [15] J. Muster, G. T. Kim, V. Krstic, J. G. Park, Y. W. Park, S. Roth, M. Burghard. Advanced Materials 12 (2000) 420-424.
- [16] N. Ferrer-Anglada, J. A. Gorri, J. Muster, K. Liu, M. Burghard, S. Roth, Mater. Sci. and Engineering: C 15(2001)237-239.

- [17] M. Zeng, H. Yin, K. Yu, Chem. Eng. J. 188(2012)64–70.
- [18] T. Ivanova, A. Harizanova, T. Koutzatova, B. Vertruyen, Mater. Lett. 64(2010)1147–1149.
- [19] M.H. Mamat, M. Z. Sahdan, Z. Khusaimi, M. Rusop, in Proceedings of the International Conference on Electronic Devices, Systems and Applications (ICEDSA'10), 2010, pp.408–411.
- [20] A. Talledo, C. G. J. Granqvist, J. Appl. Phys. 77(1995)4655–4666.
- [21] V. Naydenov, L. Tosheva, J. Sterte, Microporous Mesoporous Mater. 55 (2002) 253–263.
- [22] D.R.W. Briigel, An introduction to Infrared Spectroscopy, New York, 1962.
- [23] N. Nagarani, J. Photon. Spintron. 12 (2013)19–21.
- [24] N. Senthilkumar, M. Sethu raman, J. Chandrasekaran, R. Priya, Murthy Chavali, R.Suresh. Mater. Scien in Semi. Processing 41(2016) 497-507.
- [25] V.K.Saraswat, K.Singh, N.S. Saxena, V.Kishore, T.P.Sharma, P.K.Saraswat. Curr.Appl.Phys.6 (2006).
- [26] Y.Tominaga, S.Asai, M.Sumita, S.Pamero, B.Scrosati, J.Power Source 0146 (2005)402-406.